

## **TRIAXIAL TENSION TESTS ON COMPACTED KAOLIN**

**E.K. Berdie<sup>1</sup>**

### **SYNOPSIS**

This paper describes a technique of carrying out triaxial tension tests on compacted kaolin specimens based on modifications of the conventional triaxial test. The tests were conducted on specimens having a central stem of reduced diameter. The specimen preparation covered a wide range of initial conditions, and the results indicated that while the pore pressure response and dilatancy were dependent on the compaction water content and overconsolidation ratio, the ultimate tensile strength remained constant with a value of about 20kPa. This suggested the possibility of formulating yielding behaviour of compacted clays in tension with a limiting tension criteria defined by the concepts of fracture mechanics. Also the conduct of the test will allow the examination of the experimental data in terms of established constitutive relations under axi-symmetric stress systems.

### **INTRODUCTION**

Soil compaction has been employed as a standard construction practice to improve the stability and deformation characteristics of embankments as well as a seepage control measure in the cores of dams. Extensive research work exists in the literature aimed at setting guidelines to ensure the satisfactory performance of the materials consigned to the embankment under shear and compressive loads, e.g., increases in stiffness have been associated with compaction in the vicinity of the optimum moisture content (OMC). The design practices commonly adopted in dealing with the stability and deformation characteristics of compacted clays have, for many years, ignored the tensile capacity of these materials. Tensile stress regimes are however encountered in many structures such as, rigid and flexible layered pavements, in the cores of dams and in the upper parts of natural and man-made slopes. When the generated tensile stresses in such systems exceed the tension capacity of the material, the performance and integrity of the structure are endangered. Such a phenomenon may manifest in pavement systems as visible cracks and in dams as progressive erosion leading to piping failure. The problem in dams is made more difficult in the sense that

---

<sup>1</sup>Lecturer, PNG University of Technology, Private Mail Bag, Lae, Papua, New Guinea.

failure of the structure many will be established before the presence of the cracks are evident. Covarrubias in 1969, for instance, identified the location of tensile zones which may result in cracks designated as open crack modes in the bottom of embankments founded on softer materials, the upper zones of earth dams near the abutments and in the interior of dams near abrupt changes in the slopes of the abutments.

Research into the development of tensile stresses in soils which can translate into crack formation has developed on two fronts, viz., the generation of tensile stress-strain data based on laboratory and field tests, and the use of the test data in analytical modeling of the material behaviour under tensile stress fields. Most of the test procedures aimed at extending the behaviour of soils into the tensile stress sector are adapted from tests on brittle materials such as rocks and they can be broadly classified under the following headings:

- Direct tension tests, e.g., Tschebotarioff et al (1953) and Hasegawa and Ikeuti (1964).
- Indirect tension tests such as the Brazilian test, the Double punch test, Beam tests and Model tests with discontinuous foundations (e.g. Moore and Hor 1984).
- Triaxial tension tests, e.g., Bishop and Garga (1969), Al-Hussaini (1981).

A comprehensive review of the test methods is outside the scope of this paper and the interested reader is referred to Al-Hussaini and Townsend (1973) and Berdie (1989).

Realistic constitutive models to characterise tensile behaviour of materials are scarce. In addition suitable analytical techniques to model crack tip propagation are difficult to perform using finite element methods. This paper e.g., Clough and Woodward (1967), Covarrubias (1969), Berdie and Hoadley (1987). Most of these analyses unfortunately, are not refined enough to predict the mechanisms of actual crack formation, partly because of the lack of test data that describes both the strength and stress-strain behaviour of soils under the appropriate stress regime.

Realistic constitutive models to characterise tensile behavior of materials are scarce. In addition suitable analytical techniques to model crack tip propagation are difficult to perform using finite element methods. This paper presents a detailed description of the use of a conventional triaxial equipment for the evaluation of the tensile characteristics of compacted kaolin.

The experimental techniques follow the procedures attributed to Bishop and

Garga (1969). A major criticism leveled against the type of tension test described herein lies in the proportioning of strains in test specimens with non-uniform cross-section. This research work examines this effect. The test procedures however, offer the advantage of examining the tensile stress-strain behaviour of soils within the framework of established constitutive relations under an axi-symmetric stress system.

### TRIAXIAL TENSION TESTS - A REVIEW

The first reported tension test on soils in the triaxial equipment is attributed to Conlon (1966). The conduct of this experiment essentially conforms to an uniaxial tension test. Bishop and Garga (1969) demonstrated the feasibility of performing tension tests in the triaxial equipment by employing specimens with reduced central sections. Al-Hussaini (1981) also performed tests using the triaxial set up in which failure mechanisms were achieved under a stress system with one of the principal stresses being tensile in character. This latter work employed hollow cylindrical specimens. Although this test method is effective in the determination of tensile soil properties, the complexities associated with specimen formation, strain measurements and equipment requirements cannot be overlooked. Another major shortcoming of this particular test method lies in the use of elastic theory for the data reduction. Soils under tensile stress fields have been shown to exhibit non-linear behaviour, e.g. Ajaz and Parry (1975). The advantages of the triaxial tension test described herein over other tension tests are:

- The required equipment is a standard one commonly used in soil testing, with only minor modifications similar to those required for the conduct of triaxial extension tests.
- The test specimens are more manageable in size unlike the specimens required for direct tension tests, e.g., Tschebotarioff (1953).
- The experimental set up has facilities to independently monitor and control the pore water and air pressures if required.
- It avoids the complications associated with sample gripping typical of direct tension tests.
- There are no assumptions regarding the stress-strain behaviour in the data reduction process. This latter consideration is a characteristic of indirect tension tests.
- As mentioned earlier, the loading pattern can fit into the framework of existing elasto-plastic soil models.

## TESTING EQUIPMENT REQUIREMENTS

The testing equipment used in this study consists of a standard triaxial testing machine capable of accommodating 50mm diameter test specimens. This equipment was modified to various degrees in order to conduct extension type tests. The modifications are illustrated in Fig. 1. The top cap of the specimen was fabricated in such a manner that coupling of the top loading ram can be effected outside the cell chamber, the coupling being such as to transmit axial extension to the test specimen. A provision was made for a universal joint between the connector to the specimen top cap and the loading ram. This was a convenient way of eliminating eccentric axial load which was maintained by a 445N capacity load cell located outside the cell chamber. The base of the triaxial cell was secured to the loading platen of the equipment by clamping screws.

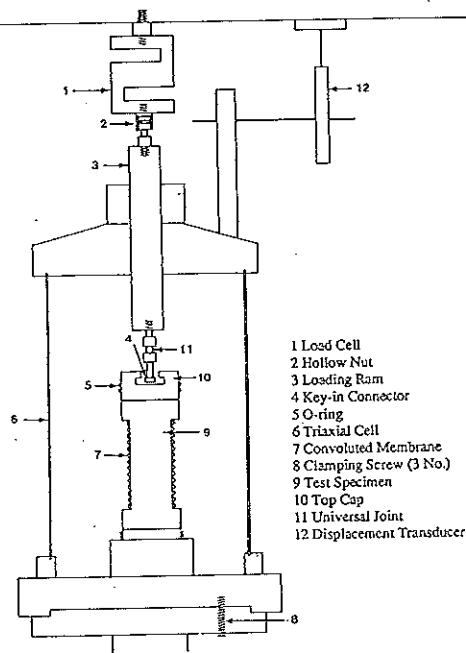


Fig. 1 Experimental Set-up

## TRIAXIAL TENSION TESTS

Displacements were monitored by an external linear variable displacement transducer (LVDT), as shown in Fig. 1, in addition to optical measurements made by sightings on targets fixed to the test specimen. The test specimens were enclosed in specially fabricated convoluted latex membranes, the convolutions extending over the critical section of the test specimen which will experience tensile stresses. When completely unfolded, the convolutions extend by approximately 27.5 mm. This value is far in excess of the axial deformations of the test specimens recorded at failure. The chamber and back pressures were maintained by a standard self compensating mercury system described by Bishop and Henkel (1962). The cell and pore pressures were monitored by *Druck* type transducers whilst volume change response was recorded by an electronic volume change unit (model number EL 26-488). With the exception of the vernier microscope which was used to optically evaluate strains, all the other monitoring devices were connected to an automated data logging equipment.

## SPECIMEN GEOMETRY AND LIMITING CONDITIONS

In a standard triaxial extension test in which failure is brought about by a gradual reduction in the axial stress while maintaining the cell pressure, there is a lower limit on the level of the cell pressure to ensure that the top cap does not detach from the specimen before failure is manifested. This threshold of cell pressure is governed by the dimensions of the test specimen. This condition is also applicable to the tension tests described in this paper. Referring to Fig. 2 which depicts a schematic section of the test specimen used in this work, the lower limit of the cell pressure is expressed by Eqn. 3. In the tension test reported herein, there is an additional restriction on the upper limit of the confining pressure which is governed by the shear strength characteristics of the material. This point is best illustrated by referring to Fig. 3 where the choice of the confining pressure is such that tensile failure is attained with the test paths confined to stress regimes below the limiting line defining the shear failure envelope, e.g., test specimens D and C in Fig. 3. It is noted that because of the conduct of the test, there is a rotation of the principal stress directions such that the axial stress becomes the minor principal stress ( $\sigma_3$ ) and the intermediate stress equals the major principal stress ( $\sigma_1$ ) defined by the confining pressure. Referring to Fig. 2, the average stresses in the various section of a typical tension test specimen are

$$\sigma'_{1E} = \sigma'_r - \frac{T}{A_E} \quad \dots 1$$

$$\sigma'_{1c} = \sigma'_r - \frac{T}{A_c} \quad \dots 2$$

where

$\sigma'_r = \sigma'_1$  = the effective cell pressure

T = applied tensile load

$A_E$  = cross-sectional area of the enlarged ends

$A_c$  = cross-sectional area of the reduced central section

$\sigma'_{1E}$  = the effective axial stress in the enlarged ends

$\sigma'_{1c}$  = the effective axial stress in the central section.

The limiting value of T in the enlarged ends is reached when

$$\sigma'_{1E} = 0$$

or

$$\sigma'_{1c} = -\sigma'_r \left[ \frac{A_E}{A_c} - 1 \right] \quad \dots 3$$

Based on the above considerations and experimental investigations, the effective confining pressures were limited to the range 50 to 120kPa.

### CHOICE OF MATERIAL AND SPECIMEN PREPARATION

The tests were carried out on compacted samples of commercial kaolin which came in a powdered form at moisture contents between 1 and 2%. The index properties of the material are LL = 52.3%, PI = 22.8%, SG = 2.60; Proctor OMC and MDD are respectively 26.8% and 1.467g/cm<sup>3</sup>. Kaolin was used because it is a common clay mineral which is amenable to easy mixing to any desired water content to produce a homogeneous material. Kaolin also exhibits relatively high permeability with low thixotropic hardening. The latter features allow comparatively quick dissipation of excess pore water pressures under loading and minimal variations in strength with respect to time after specimen preparation.

Sub-batches of the material were mixed with predetermined quantities of distilled water and stored for seven days to cure. Allowance was made for moisture loss during mixing and curing in order to meet the target moisture contents shown in Table 1. The samples were then compacted at equivalent Standard Proctor energy in a mould fabricated to conform to the internal

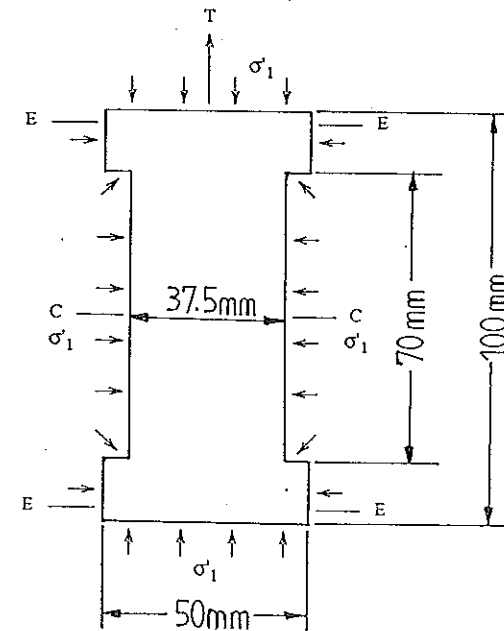


Fig. 2 The Test Specimen

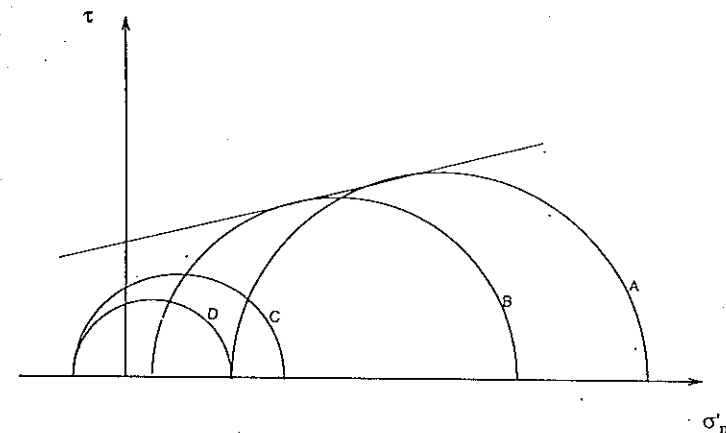


Fig. 3 Tensile and Shear Failures

dimensions of a CBR mould. The compaction was done by a dynamic method and involves subjecting three layers of the cured material to 30 blows (per each layer) of the modified AASHO hammer. The CBR mould was an experimental expedience which allows compacted specimens to be retrieved orthogonally to the direction of the compaction planes. These specimens were machined to conform to cylindrical triaxial test specimens measuring 50mm in diameter and 100mm in length. Comparisons made between the densities achieved in the CBR mould and those obtained at Standard Proctor energy (AS 1289 – 1977) showed good agreement.

Table 1 Soil Properties Achieved on Compaction

Compaction condition	Moisture content before test (%)	Dry Unit Weight ( $kNm^{-3}$ )	Void ratio	Degree of saturation (%)
A	20.61	13.283	0.919	58.32
B	21.87	13.777	0.852	66.79
C	25.43	14.233	0.792	83.48
D	26.75	14.393	0.772	90.10
E	30.12	13.863	0.840	95.72
F	35.82	12.967	0.967	93.33

The sampling direction was a critical consideration arrived at after trials on specimens retrieved with the major cylindrical axis parallel to the direction of compaction gave specimens with inherent discontinuities at the interfaces of the compaction layers. Triaxial tension tests carried out on these trial specimens were found to fail at the zones conforming to the compaction discontinuities. Scarification of the tops of successive compacted layers in order to achieve adequate bonding was not effective in eliminating this problem. It was therefore concluded that any tensile properties derived from such specimens will be related closely to the degree of bonding achieved between the various compacted layers. It is pertinent to note that the direction of sampling followed in this work in relation to the tensile failure mechanism can be characterised by Mode I crack formation (the opening mode) described by Paris and Sih (1964). The existence of Mode I cracks in compacted embankments has been discussed by Covarrubias (1969). These cracks are designated transverse-exterior and longitudinal-exterior by Covarrubias or simply as transverse cracks by Lowe (1970).

## TRIAxIAL TENSION TESTS

Samples with nominal dimensions 53mm in diameter and 120mm in length were recovered from the compaction mould using stainless steel sampling tubes. A portable lathe was used in turning the specimens to the desired shape shown in Fig. 2. The lathe was assembled from the motor of a commercially available variable speed drill mounted in such a manner as to rotate the cylindrical specimens with the major axis in a horizontal plane relative to a cutting tool which was hand controlled by two screw feed systems. One screw feed controlling the lateral movement whilst the other regulated the cutting depth. The speed of specimen rotation was maintained by a variable output transformer, with maximum rotation speed kept to 30 revolutions per minute in order to reduce possible sample disturbance that may arise from induced centrifugal forces. The turning operation which took an average of 15 minutes was done in a controlled environment with ambient temperature of  $22 \pm 1^\circ$ . Changes in density and moisture content after the machining process were observed to be minimal.

## TESTING PROCEDURES

Four 1cm wide filter strips were symmetrically installed along the longitudinal perimeter, in addition to filter discs at the top and bottom of the specimens. The axial filter strips were installed in four segments, the sections slightly overlapping each other. This measure was aimed at reducing likely filter paper restraint during axial extension. The specimens were enclosed in the convoluted rubber membranes and sealed to the top cap and bottom pedestal by means of rubber O-rings in the conventional manner and saturated under a back pressure of 300kPa. This level of back pressure achieved 95 to 100% degree of saturation estimated on the basis of the B-value method. The saturation process was aimed at simulating long term field conditions where the material is allowed to equilibrate under steady state seepage or hydrostatic pressures. Following back saturation, the test specimens were consolidated to the desired levels of isotropic stress, and depending on the stress patterns employed for the purposes of these tests, the specimens are designated normally or over consolidated. For instance, a test specimen which was initially consolidated at 380kPa and subsequently allowed to equilibrate at a lower spherical pressure of 50kPa is considered an over consolidated material with an over consolidation ratio of  $\frac{380}{50} = 7.6$ . It was necessary to introduce the chamber pressure prior to coupling the deviator stress monitoring device to the specimen top cap. This was necessary because the equipment fabrication was such that the chamber pressure imposes an upthrust on the loading ram which

would have introduced premature stresses in the specimens had the coupling been engaged before the application of all-round pressure. A controlled strain rate of 0.002mm/min was maintained throughout the testing. The choice of this loading rate was made on the basis of 95% minimum pore water dissipation/equalisation during loading.

### DATA REDUCTION

#### Examination of pore pressures

The geometrical configuration of the test specimens warrants the examination of the differences in pore pressures that might exist in the ends and the reduced central section. Using a flexible tubing similar to that employed in the pore pressure measuring device in a conventional triaxial test, a small incision made in the rubber membrane permitted the pore water pressures generated under undrained loading in the middle periphery of the test specimen to be monitored in addition to the pore pressures developed at the enlarged ends. The incision made in the membrane was sealed with a silicone based rubber sealant of commercial name *Loctite* prior to testing. This investigation was carried out on a couple of the specimens and the observations revealed insignificant differences in the pore water pressures mobilised at these three locations throughout the loading process. This manifests the effectiveness of the installation of the periphery filter drains described earlier in the even distribution of pore pressures over the length of the specimens. Pore pressure records for all the test specimens were therefore based on measurements made at the ends of the specimens.

#### Axial and volumetric strain proportioning

The axial strain records of the external LVDT is a direct measurement of the changes in the axial deformation of the total specimen. Due to the stress differences introduced by the non-uniform cross-section of the specimens, the average deformations in the reduced central section will be different from those at the enlarged ends. Consequently, observations of the total sample deformation are not liable to reflect the behaviour of the reduced central section. To address this issue, measurements made by a vernier microscope, monitoring the displacements of targets fixed to the central gauge section of the test specimens, were compared with the records of the LVDT.

The volumetric strains developed under the application of the deviatoric stresses in tests where drainage is allowed will also require corrections. To

examine the response of the stress-strain paths, the test results were analysed subject to three different assumptions regarding the volumetric strain proportioning. These assumptions listed below, are made clearer with the aid of Fig. 4.

- The volumetric deformations are solely from the contribution of the cylindrical portion extending over the length of the reduced central section (Assumption 1, Fig. 4 (a)).
- The volumetric strains are entirely restricted to the portion of the test specimens having the same diameter as the reduced central stem but extending over the full height of the specimens (Assumption 2, Fig. 4 (a)).
- The volumetric deformations are uniform over the entire specimen volume (Assumption 3, Fig. 4 (a)).

The above considerations were coupled with the axial deformations records discussed earlier to produce three different analyses thus:

- Axial deformations of the central gauge section and the volumetric deformations corresponding to Assumption 1.

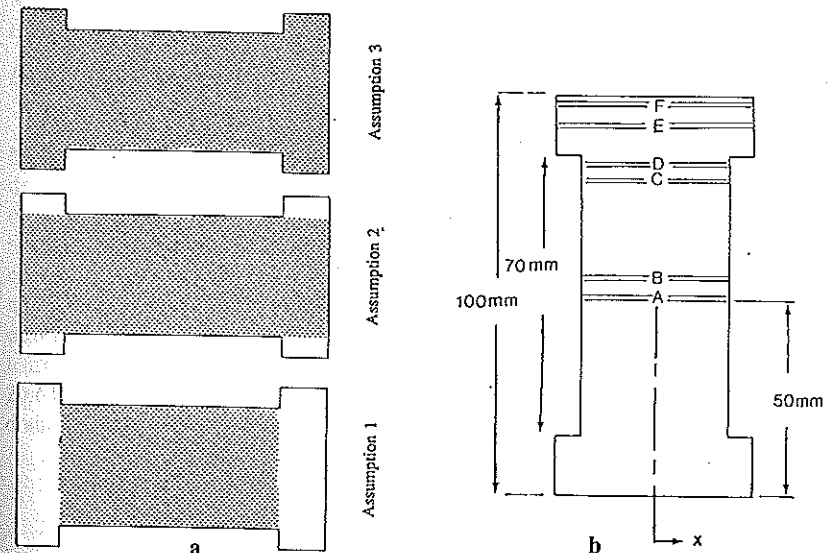


Fig. 4 Definitions of Participating Volumes and Stress Profile Zones

- Axial deformations of the central gauge section and volumetric deformations corresponding to Assumption 2.
- Axial deformations records from the LVDT and uniform volumetric changes of the total test specimen.

These three methods of analytic considerations, hereafter referred to respectively as Analysis 1, 2 and 3, formed the basis for the typical stress-strain plots presented in Fig. 5. These analytical features are refinements to the pioneering work of Bishop and Garga (1969) and are directed at resolving the criticism leveled at this test method. A discussion of the effect of these considerations is outlined in a subsequent section.

#### Finite element procedures

A finite element procedure based on the Abaqus computer package (Hibbitt et al 1984) was utilised to further evaluate the deformation and stress profiles within the test specimens. The model definition conforms to the dimensions of the specimens employed in the experimental phase, whilst the material description was idealised by a linear elastic behaviour with Young's

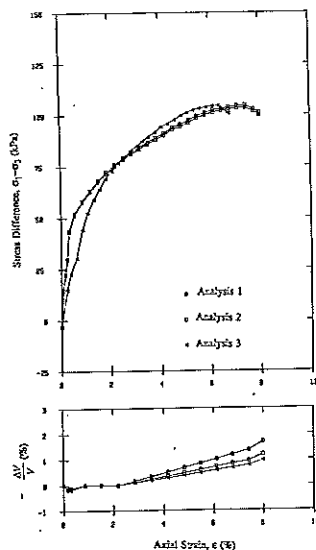


Fig. 5 Stress-Strain Plots for Specimen NCD-T-D90

modulus and Poisson's ratio of 5MPa and 0.3. The loading configuration adopted was tailored to simulate experimental conditions corresponding to an axi-symmetric solid initially in equilibrium under a spherical pressure of 100kPa, upon which incremental axial stress reductions, with a maximum value of 25kPa in the reduced central stem, were superimposed. Expressing the axial strains based on the analytical deformations predicted from the overall specimen length as a ratio of the corresponding values developed in the central stem section gave a value of 0.86. By changing the diameter of the central stem from 37.5 to 30.0mm, the corresponding ratio of axial strains dropped to 0.84. These observations suggest non-uniformity in the transmitted stresses within the test specimens. It is therefore instructive to examine the stress profiles developed in the models as done in Fig. 6. Because of the bi-directional symmetry of the model about its mid point, the information in this figure is presented for the top right quarter of the model. The zones for the profiles depicted in Fig. 6 are shown in Fig. 4 (b). The stress fields in the region bounded by zones A and C were observed to be remarkably uniform until one approaches zone D when changes in the stress components are evident. The linearity in stresses decreases further in the enlarged ends (refer Fig. 6 (d)).<sup>1</sup> On the basis of these findings, only the experimental data for the test specimens which manifested failure between zones A and C were considered in the results discussed hereafter.

#### Examination of test data

In the specimen numbering adopted in this work, the initial set of letters, NCD, NCU, OCD and OCU respectively refer to normally consolidated drained, normally consolidated undrained, overconsolidated drained and overconsolidated undrained test conditions. The second letter T signifies tensile testing regime and the last set of letters corresponds to the compaction condition (governed by the moulding water content) to which is appended the nominal effective chamber pressure at which the test was performed. For example, specimen NCD-T-A50 denotes a normally consolidated drained tension test at compaction condition A (average moulding water content = 20.61%) tested at a nominal effective confining pressure of 50kPa with drainage being allowed during the application of the deviatoric stresses.

<sup>1</sup> For brevity, some of the profiles are omitted and the reader is referred to Berdie (1989) for a complete record.

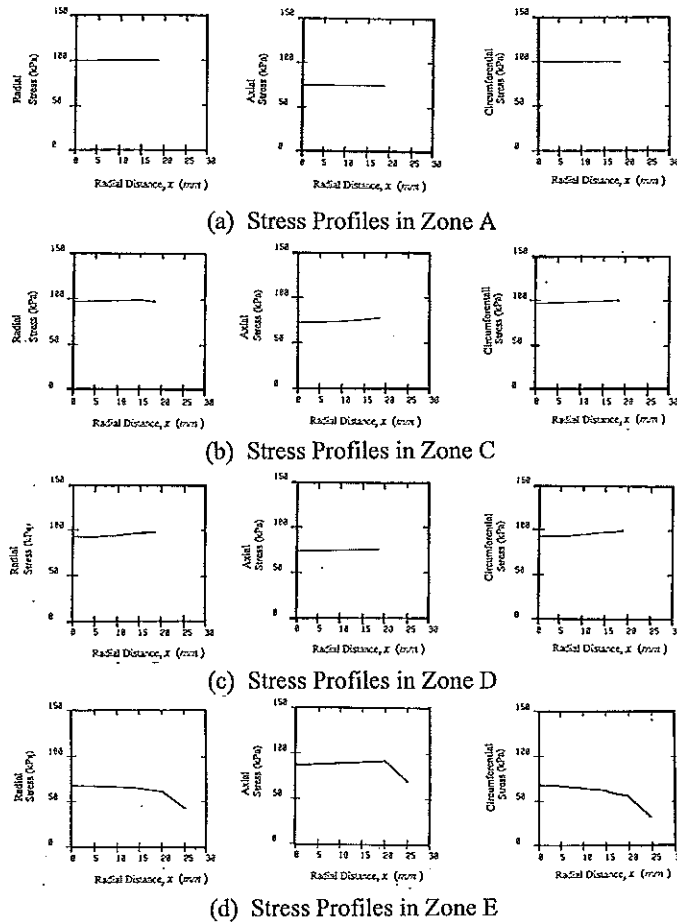


Fig. 6 Predicted Stress (37.5mm Diameter Central Stem)

*Stress strain characteristics*

A typical stress-deformation profile, under conditions where drainage was permitted, is presented in Fig. 5 for the three methods of analysis discussed previously. The salient observations made from several of these stress-strain plots are as follows. The peak stress differences and consequently, the failure tensile strengths are insensitive to the three methods of data reduction.

Indeed, the disparities in the computed peak stress differences are so small that there seems to be no justification for the amount of time expended and the difficulties associated with strain monitoring in the central stem section if strength considerations are the sole purpose of an investigation of this nature. With regards to failure strains, the various methods of analysis yielded significantly dissimilar results. The computed volumetric strains at failure decrease in the order Assumptions 1, 2, 3. It is reasonable to expect this pattern since the participating specimen volumes in the computations also increase in the same order as the volumetric strains. The strains computations based on the external LVDT observations were also noted to be generally lower than the results derived from the records of the vernier microscope. This trend is consistent with the inferences made from the numerical methods discussed earlier, i.e., the transmitted stresses and corresponding strains are higher in the reduced stem. Also, the assumption underlying the strains based on the overall deformation of the specimen is that of uniformity of stresses. This assumption will have an effect of decreasing the average computed strains. The general trend in volumetric strain response is that of a continual specimen dilation with increases in axial strain. This pattern was consistent for all three methods of analysis.

*Pore water pressure response*

In Fig. 7, the pore pressure variations are represented as functions of the axial strains for the test specimens initially consolidated at nominal effective pressures of 50 and 100kPa. The examination of these results were carried out at compaction conditions A (-6% of OMC), C (OMC) and F (+9% of OMC). Conditions A and F are at the extremes of the compaction water contents of general interest in the field. It is reasoned that the examination of these conditions will highlight the differences in behaviour with respect to the fabrics obtained from dry and wet of the OMC conditions. Although all the specimens exhibit a general trend of dilation, it is noted that dry of OMC specimens mobilised higher suction values than the wet of OMC specimens subjected to similar stress histories prior to loading. The highest negative pore pressures are associated with conditions at the OMC. On the examination of compression and swelling characteristics for the test specimens compacted at equivalent Standard Proctor energy, Berdie (1989) observed higher changes in specific volumes per unit increase/decrease of isotropic pressure for the test specimens moulded on the dry side of the OMC when compared with the corresponding behaviour of specimens moulded wet of OMC. It can therefore be inferred that the consolidation process prior to the application of the deviatoric



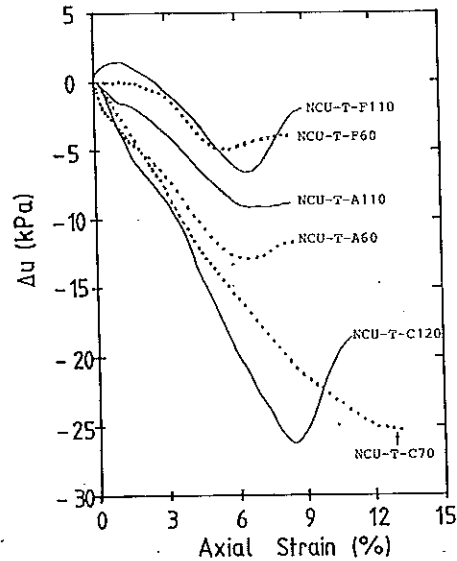


Fig. 7 Pore Pressure Response

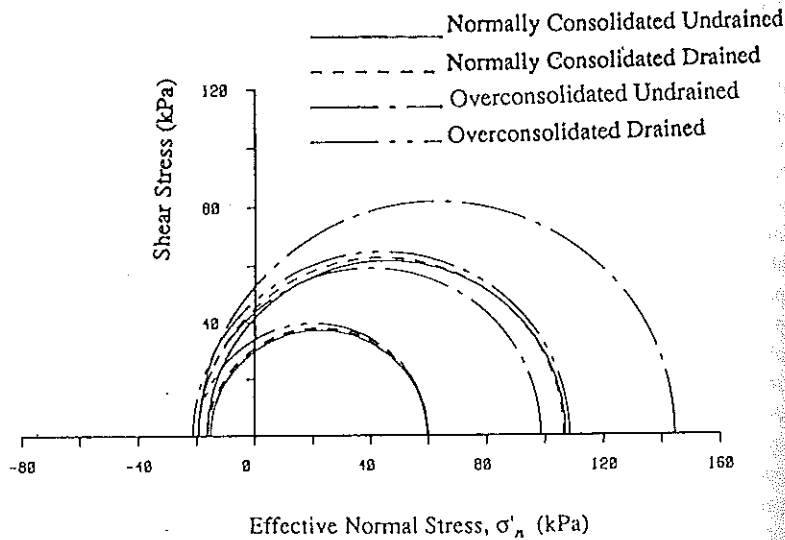


Fig. 8 Effective Mohr Circles at Compaction Condition F

stresses will increase the degree of packing for specimens moulded at condition A than for specimens at condition F although comparable densities were achieved on initial specimen compaction at these two conditions. This increased density for the dry of OMC compacted specimen and the inherently higher densities at compaction conditions in the vicinity of the OMC will account for the propensity of these specimens for an increased water demand during loading. These observations support the existing knowledge pertaining to differences in engineering behaviour with respect to compaction on the dry and wet side of the optimum water content. The pore pressure changes during the tests are generally consistent with the inferences drawn from volume change behaviour in drained tests discussed earlier. That is, if volume increases occur during drained loading, it stands to reason that pore pressure decreases will take place in undrained tests.

*Strength properties*

Table 2 contains a summary of the critical values from a total of 42 tests. The information in this table are based on the results from Analysis 1. Representing the ultimate tensile stresses for the various conditions in terms of the effective Mohr circles typified by Fig. 8, it was observed that the tensile

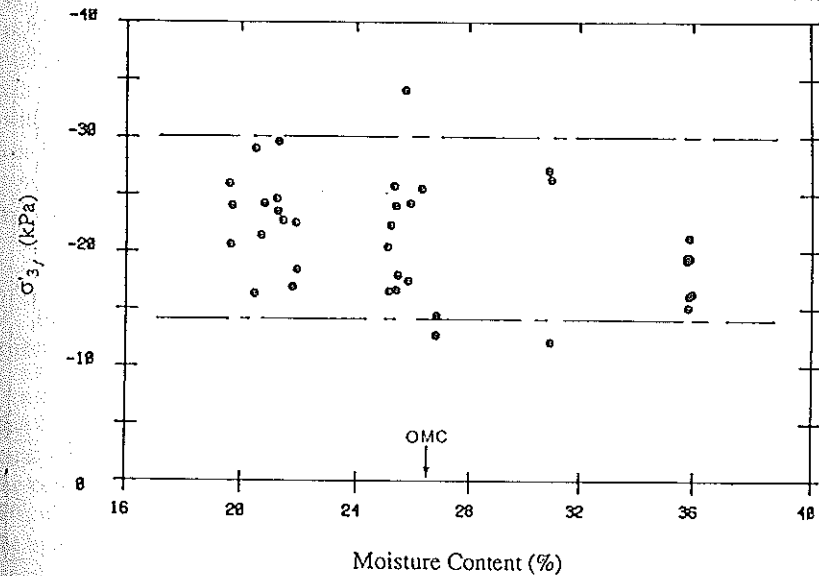


Fig. 9 Variation in Tensile Stresses at Failure

Table 2 Summary of Test Results

Specimen No.	$\sigma'_{1f}$ (kPa)	$\sigma'_{3f}$ (kPa)	$\epsilon_f$ (%)	$E_i$ (kPa)	$\left(\frac{\Delta v}{v}\right)_f$ (%)	$\Delta u_f$ (kPa)	$v_f$	OCR
NCD-T-A50	51.2	-25.9	9.30	6131	1.90	-	1.998	1
NCD-T-A70	73.2	-20.6	10.91	5672	3.32	-	1.975	1
NCD-T-A95	95.0	-24.0	9.21	5182	0.24	-	1.917	1
NCU-T-A60	59.8	-22.7	5.68	2863	-	12.1	1.913	1
NCU-T-A110	108.1	-23.5	5.76	6392	-	-9.1	1.994	1
OCD-T-A50	50.8	-24.2	9.63	2606	3.80	-	1.912	7.5
OCD-T-A53	53.9	-21.4	11.25	2078	3.56	-	1.932	6.0
OCD-T-A54	54.4	-16.3	7.47	3008	3.26	-	1.950	5.6
OCD-T-A100	102.6	-29.0	10.84	5207	2.96	-	1.890	3.0
OCU-T-A50	106.7	-29.6	10.38	5087	-	-51.7	1.876	4.0
OCU-T-A100	154.4	-24.6	7.27	7879	-	-47.1	1.882	2.0
NCD-T-B70	70.6	-22.5	8.10	2897	2.97	-	1.991	1
NCD-T-B90	87.1	-18.4	7.56	5012	1.19	-	1.947	1
NCD-T-B100	96.7	-16.9	7.14	6680	1.07	-	1.920	1
NCD-T-C80	75.7	-22.3	7.67	5433	1.13	-	1.938	1
NCD-T-C110	109.7	-20.4	9.90	4632	0.36	-	1.909	1
NCD-T-C120	121.8	-16.5	9.39	5243	1.19	-	1.906	1
NCU-T-C70	73.4	24.0	8.29	3255	-	-20.8	1.954	1
NCU-T-C120	126.1	-25.7	8.64	5150	-	-28.1	1.900	1
OCD-T-C55	55.4	-34.1	6.76	8602	3.62	-	1.885	7.3
OCD-T-C55R	55.7	-24.2	10.61	2005	4.10	-	1.905	5.6
OCD-T-C110	107.1	-17.4	6.95	14393	2.63	-	1.895	3.0
OCU-T-C50	96.4	-16.6	5.72	4772	-	-40.6	1.891	4.0
OCU-T-C100	150.8	-17.9	7.64	6059	-	-43.2	1.866	2.0
NCD-T-D65	65.2	-25.5	6.91	7731	1.67	-	1.966	1
NCD-T-D90	90.2	-14.4	7.44	9987	0.95	-	1.920	1
NCD-T-D110	113.5	-12.7	7.31	14540	1.19	-	1.907	1
NCD-T-E60	67.7	-27.1	6.89	7419	3.15	-	1.906	1
NCD-T-E70	73.2	-26.3	6.42	6096	0.56	-	1.943	1
NCD-T-E100	98.0	-12.1	5.48	6702	0.37	-	1.903	1
NCD-T-F60	60.1	-16.1	7.16	7630	0.24	-	1.963	1
NCD-T-F110	106.3	-19.2	6.71	9809	0.12	-	1.899	1
NCU-T-F60	59.3	-15.1	5.53	4107	-	-5.9	1.956	1
NCU-T-F110	107.1	-16.3	6.04	23497	-	-5.2	1.907	1
OCD-T-F60	59.9	-19.5	6.55	13728	2.28	-	1.899	5.5
OCD-T-F110	108.3	-21.2	5.15	5686	1.07	-	1.861	3.0
OCU-T-F60	98.6	-19.5	4.51	12819	-	-42.4	1.892	4.0
OCU-T-F110	144.4	-19.4	4.48	6185	-	-40.4	1.870	2.0
NCD-T-A60*	63.0	-16.0	9.45	-	0.37	-	1.952	1
NCD-T-A70**	73.2	-19.6	4.41	-	0.83	-	1.950	1
Slurry***	123.8	-21.2	12.2	8200	-	-9.1	2.035	1
Slurry***	122.8	-13.1	7.6	3800	-	-21.8	2.019	1

\* Central diameter of specimen = 37.5 mm; \*\* Central diameter of specimen = 30.0 mm; \*\*\* Tension test for kaolin reconstituted slurry.

TRIAXIAL TENSION TESTS

strengths at failure were approximately the same, irrespective of whether the test specimens were normally consolidated or over consolidated. The failure tensile stresses are represented as a function of the initial moulding water content in Fig. 9. The mean and standard deviation of the failure tensile stresses in this figure are, respectively -20.0kPa and -4.9kPa. The effect of reducing the central stem diameter from 37.5 to 30.0mm whilst maintaining the other dimensions was also examined (refer specimens NCD-T-A60 and NCD-T-A60 and NCD-T-A70 in Table 2). For all practical purposes the computed failure stresses for these two specimens are similar. Table 2 also contains test data on specimens prepared from a slurry of the same batch of kaolin material. These specimens were reconstituted in a Rowe cell to an initial moisture content of 50.8%. The inclusion of this is for the purposes of comparison. The ultimate failure stresses of these specimens also show very little dependence on the confining pressures examined. These observations concur with the findings of Bishop and Garga (1969) based on similar testing procedures on London Blue clay under effective confining pressures of the order of 20 to 70kPa. According to the Griffith theory, provided the value of the major principal stress (confining pressure) does not exceed three times the tensile strength of the material, the tensile stresses at failure should be independent of the effective major principal stress (Hoek 1965). It therefore appears that the Griffith crack theories offer some prospects in describing the cracking problem in situations where one or more of the principal stresses are tensile in character. It is conceptually and intuitively appealing to combine the Griffith fracture models with established constitutive relations for soils under axi-symmetric loading conditions (as pursued in this work) in order to develop unifying yielding and tensile crack formation theories which can represent the behaviour of clays in general under tensile stress regimes.

CONCLUSIONS

Based on the experimental work and the discussions presented, the following conclusions are drawn:

1. By employing standard triaxial extension techniques and specimens that have been machined to have a central stem of reduced diameter, it was established that tensile stresses could be developed in the test specimens without the complications of the end effects associated with direct tension tests. One difficulty of the test method pursued in this paper lies in the establishment of the appropriate axial strains as the strains are not uniform over the specimen length. The axial strains had only a small influence on the axial stresses

calculated after correction for the measured volume changes.

2. Under the application of the deviatoric stresses, all the specimens exhibit dilatant behaviour; the degree of dilation being dependent on the compaction water content. Specimens compacted in the vicinity of the optimum moisture content developed the largest suction, but specimens compacted dry of the optimum water content mobilised greater negative pore pressures than those compacted wet of the optimum water content.

3. In terms of the tensile carrying capacity, the observations indicate a limiting tension criteria; the computed ultimate stresses being independent of the confining pressure and the stress histories of the test specimens.

4. The possibility of formulating the yielding behaviour of compacted clays in tension by the prescriptions of existing constitutive models, e.g., Critical state formulations, with a limiting tension criteria defined by the concepts of fracture mechanics is suggested.

#### ACKNOWLEDGEMENTS

The work described in this paper was carried out in the Department of Civil Engineering, The University of Melbourne. The writer gratefully acknowledges the financial and technical assistance from this institution and the advice received from Dr. P. J. Hoadley and other members of the soil mechanics group at The University of Melbourne.

#### REFERENCES

- AJAZ, A. and PARRY, R. H. G., Stress-Strain behaviour of two Compacted Clays in Tension and Compression, *Geotechnique* 25, 3 (1975), 495-512.
- AL-HUSSAINI, M. M. & TOWNSEND, F. C., *Tensile Testing of Soils A Literature Review*, U.S. Army Engineer Waterways Experiment Station Vicksburg, Mississippi, May 1973.
- AL-HUSSAINI, M. M., Tensile Properties of Compacted Soils, in *Laboratory Shear Strength of Soils*, ASTM STP 740, R. N. YONG and F. C. TOWNSEND (Editors), 1981, p. 207-225.
- BERDIE, E.K. & HOADLEY, P.J., Finite Element Predictions of Deformation Characteristics of Compacted Soils, *Proc. Fifth Int. Conf. in Australia on Finite Element Methods*, 1987, p. 139-144.
- BERDIE, E.K., *The Behaviour of Compacted Kaolin in the Tensile Stress Domain*, PhD Thesis, The University of Melbourne, 1989.

#### TRIAXIAL TENSION TESTS

- BISHOP, A. W. and HENKEL, D. J., in *The Measurement of Soil Properties in the Triaxial Test*, Arnold, London, 1962. Second Edition.
- BISHOP, A.W. & GARGA, V.K., Drained Tension Tests on London Clay, *Geotechnique* 19 (1969), p. 309-313.
- CLOUGH, R. W. & WOODWARD, R. J., Analysis of Embankment Stresses and Deformations, *Proc. ASCE Journal of Soil Mechanics and Foundations Division* 93, SM4 (1967), p. 529-549.
- CONLON, R. J., Landslide on the Toulmoustou River, Quebec, *Canadian Geotechnical Journal* 3, 3 (1966), p. 113-144.
- COVARRUBIAS, S. W., Cracking of Earth and Rockfill Dams; A Theoretical Investigation by means of the Finite Element Methods, *Harvard Soil Mechanics Series*, 1969.
- HASEGAWA, H. & IKEUTI, M., On the Tensile Strength of Disturbed Soils, in *Symposium on Rheology and Soil Mechanics*, Springer-Verlag, Berlin, 1964, p. 405-412.
- HIBBITT, H. D. et al, in *ABAQUS - Theory Manual*, May 1984. V4. 5.
- HOEK, E., Rock Fracture under Static Stress Conditions, CSIR Report MEG 383, 1965, South Africa.
- LOWE, J., Recent Developments in the Design and Construction of Earth and Rockfill Dams, *Transactions of the Tenth International Congress on Large Dams* 5 (1970), p. 1-28. Montreal.
- MOORE, P. J. & HOR, A. Y. T., Cracking Behaviour of Compacted Clays, *Proc. Fourth Australian-New Zealand Conference On Geomechanics*, 1984, p. 569-573. Perth, Australia.
- PARIS, P. C. & SIH, G. C., Stress Analysis of Cracks, in *ASTM STP 381*, 1964, p. 30-83.
- STANDARDS ASSOCIATION OF AUSTRALIA, *Methods of Testing Soils for Engineering Purposes*, AS 1289-1977.
- TSCHEBOTARIOFF, G. P., WARD, E. R. & DePHILLIPE, A. A., The tensile Strength of Disturbed and Recompactd Soils, *Proc. Third Int. Conf. on SMFE I* (1953), p. 207-210.